

Received: 2020.03.12

Accepted: 2020.04.23

Available online: 2020.05.18

Published: 2020.07.13

Structure Design and Optimization of the C5–C6 Cervical Intervertebral Fusion Cage Using the Anterior Cervical Plate and Cage Fixation System

Authors' Contribution:

Study Design A

Data Collection B

Statistical Analysis C

Data Interpretation D

Manuscript Preparation E

Literature Search F

Funds Collection G

AE 1,2 Jiajia Wang
BC 2 Zhihui Qian
D 3 Changlei Cui
F 4 Zhijun Guo
G 2 Luquan Ren

1 College of Agricultural Equipment Engineering, Henan University of Science and Technology, Luoyang, Henan, P.R. China

2 Key Laboratory of Bionic Engineering (Ministry of Education), Jilin University, Changchun, Jilin, P.R. China

3 Department of Anesthesiology, First Hospital of Jilin University, Changchun, Jilin, P.R. China

4 College of Vehicle and Transportation Engineering, Henan University of Science and Technology, Luoyang, Henan, P.R. China

Corresponding Author: Zhihui Qian, e-mail: zhqian@jlu.edu.cn

Source of support: National Natural Science Foundation of China (No. 51905155, No. 51675163); the Project of Scientific and Technological Cooperation between China and Italy [No. 2016YFE0103700]; and the Fundamental Research Funds of China [No. Z201105]

Background: The fifth and sixth cervical vertebra (C5–C6) is the most easily injured segment encountered in clinical practice. The anterior cervical plate and cage (ACPC) fixation system is always used to reconstruct the intervertebral height and maintain the segmental stability. The postoperative effect, such as subsidence, neck pain, and non-fusion, is greatly affected by the cervical cage structure design. This study determined reasonable structure size parameters that present optimized biomechanical properties related to the postoperative subsidence often accompanied with ACPC.


Material/Methods: Twenty bionic cages with different structural sizes (distance between the center of the cage and groove, groove depth, and groove width) were designed and analyzed based on the regression optimization design and analysis method combined with FE analysis. Because a previous study showed that greater stresses on the endplate are associated with higher risk of subsidence, the optimization object was selected as the stresses on endplate to lower it.

Results: The postoperative stresses on the endplate of all cages with bionic structure design were proved to be lower than with the original one. The optimal structure size was the distance between the center of the cage and groove=0 mm, groove depth=3 mm, and groove width=4 mm. Regression analysis found the cage with optimized bionic structural parameters resulted in a 22.58% reduction of endplate stress response compared with the original one.

Conclusions: The bionic cage with optimized structural sizes can reduce the subsidence risk, suggesting that the optimization method has great potential applications in the biomechanical engineering field.

MeSH Keywords: **Finite Element Analysis • Postoperative Complications • Prosthesis Implantation**

Full-text PDF: <https://www.medscimonit.com/abstract/index/idArt/924236>

 2688

 5

 5

 36



Background

Anterior cervical interbody fusion is widely used for decompression and fusion in patients who have severe cervical spondylosis myelopathy and intervertebral disc herniation [1,2]. Postoperative complications (postoperative subsidence and non-fusion) have attracted increasing attention [3–5]. There now exist many types of cervical interbody fusion devices, classified as transverse cylindrical structure (BAK-C Cage and Inter Fix Cage) and stand/vertical annular (AcroMed I/F Cage, SynCage, and Wing Cage). Cadaver and *in vivo* experiments showed that the vertical ring fusions have a lower postoperative subsidence rate and were conducive to fusion compared with the horizontal cylindrical ones [6–9]. Oliver et al. showed that ACPC resulted in reduced rates of subsidence, increasing rates of fusion, and lower rates of neck pain at last follow-up [10]. Moreover, Fernandez-Fairen et al. reported that the cages with plating were still in good condition at 11-years follow-up postoperatively [11]. Use of fusion cages and plates with screws can promote fusion [12]. Kettler et al. found that fusion device design greatly affects the subsidence rate [13]. The vertical ring-shaped cage is now regarded as the most reasonable design [14]. However, further research is needed to determine how fusion cage design influences postoperative outcomes.

The cage design in this study was guided by the concept of bionics, which is an interdisciplinary subject taking various scientific ideas and engineering solutions from nature. Bionics is divided into several categories: structural bionics [15], mechanical bionics [16], control bionics [17], and information bionics [18]. The human cervical intervertebral disc is an indigenous component that can be used as a natural bionic prototype. The discs contain 2 different structural elements – the annulus fibrosus and the nucleus pulposus. From the viewpoint of material mechanics, the annulus fibrosus is flexible protein, and the nucleus pulposus is a gelatinous solid that is always regarded as an incompressible material [19,20]. Cages designed using hard materials such as titanium/titanium alloy/PEEK provide sufficient mechanical support but have less flexibility compared with human tissue. To mimic the real annulus fibrosus and nucleus pulposus, a design was developed with side slotting of the titanium cage, called bionic structure, so the cage can remain flexible during structural change/modification without adding any new materials.

The research techniques applied in this study including the experimental optimization design method and the finite element (FE) method. The experimental optimization design method, such as orthogonal experimental optimization (Taguchi method), can simplify and standardize the fractional factorial experimental design, which had been applied to prosthetic design optimization [21–24]. The finite element analysis method

has been widely used to simulate the various situations of the optimization design of cages [23,24].

In the present study, we designed a bionic structure and then used the optimization design method to determine the optimal structural size based on the FE model. Firstly, based on previous studies, we made some improvement in the structural design of cages and focused on factors that change the influence of the cage bionic structures on the inner stress responses of endplates. Secondly, quadratic universal rotation design [25], which is a regression optimization design analysis method, was used to optimize the cervical cage size.

Material and Methods

Model generation

This study was follow-up research of a previous study of the influence of shape changes of cervical cages on the biomechanical properties of ACPC [26]. The previous C5–C6 FE model with fixed plate and screw was used. The model's vertebral parts included cortical bone, cancellous bone, endplates, and posterior structure. Seven ligaments were built anatomically: an anterior longitudinal ligament, a posterior longitudinal ligament, a ligament flavum, a supraspinous ligament, an interspinous ligament, a transverse ligament, and a capsular ligament. The intervertebral disc contained the nucleus pulposus and annulus fibrosus. The model's material properties – vertebra, ligaments, and annulus fibrosus – were derived from existing literature [27–29] (Table 1). The nucleus is considered as incompressible solid elements whose volume is one-third that of the disc volume [30]. The facet joints were assigned as a frictionless surface to surface contact property, as previously reported [27,31].

The cervical cage was modeled and implanted to mimic the ACPC approach. The materials for cage and fixing system were titanium alloy with a Young's modulus of 100 GPa and Poisson's ratio of 0.30 [32]. The bone graft material was set as cancellous bone with a Young's modulus of 3.5G Pa and Poisson' ratio of 0.30 [33]. The tie contact properties were assigned between C5–C6 FE model and designed cages. A uniform compressive force of 52.5 N was axially exerted on the vertebrae of C5, which imitated the gravity of the head, and a torque of 1.8 Nm was exerted to mimic the bending motion mode, while most of the nodes at the bottom of C6 were completely constrained (Figure 1). In the middle of the cage along the superior-inferior direction, there is a groove intended to mimic the cage's stiffness change in the same direction, and the specific dimensional design is shown in Figure 2.

Table 1. The material properties [23–25] set in the C5–C6 FE model.

Component	Element type	Density (Ton/mm ³)	Young's modulus (MPa)	Poisson's ratio	Cross-section area (mm ²)
Cortical bone	Trilateral	1.83E-09	12000.0	0.29	–
Cancellous bone	Tetrahedral	1.00E-09	450.0	0.29	–
posterior structure	Tetrahedral	1.83E-09	3500.0	0.29	–
Annulus	Tetrahedral	1.20E-09	3.4	0.40	–
Nucleus	Tetrahedral	1.36E-09	1.0	0.49	–
Endplate	Trilateral	1.83E-09	12000.0	0.29	–
Anterior Longitudinal ligament	Truss	1.10E-09	30.0	0.40	6.1
Posterior longitudinal ligament	Truss	1.10E-09	20.0	0.40	5.4
Ligamentum flavum	Truss	1.10E-09	10.0	0.40	50.1
Supraspinous ligament	Truss	1.10E-09	1.5	0.40	13.1
Interspinous ligament	Truss	1.10E-09	10.0	0.40	13.1
Capsular ligament	Truss	1.10E-09	10.0	0.40	46.6
Transverse ligament	Truss	1.10E-09	20.0	0.40	15.0

Procedures of the optimization method

Building the objective function

The purpose of cervical cage optimization is to find the best combination of cage parameters to obtain the lowest stress on the endplate to reduce the subsidence rate. Because the material property of human bones has been shown to be elastoplastic [34], Von Mises stress was used to analyze FE simulation output aiming to reveal the stress state of the bones and compare the cage subsidence tendencies [35].

Determining controlling factors and levels

Three key controlling factors of the cage structural dimensions were considered: the distance between the center of cage and center of the groove (represented as s), the width of groove (represented as b), and the depth of the groove (represented as h) (Figure 2). Z_i ($i=1, 2, 3$) refers to the 3 factors: s (z_1), b (z_2), and h (z_3), respectively. Among them, the positive/negative of factor $z1$ represented that the center of a groove located above/below the center of the cage. These factors, levels, and coded formula are shown in Table 2.

The experimental points calculation was based on the formula (1–3):

$$m_c = 2^p \quad (1)$$

$$m_r = 2p \quad (2)$$

$$r = m_c^{1/4} \quad (3)$$

p represents the number of the factors, $p=3$ in this study; m_c represents the two-levels for all factors full experimental point number, $m_c=2^p=8$ and m_r represents the asterisk points distributed on the coordinate axes whose number is p , $m_r=2^p=6$. r denotes the asterisk arm length, which represents the distance between asterisk points and the center point. r is the undetermined parameter, used to obtain the orthogonality and rotational property; it can be determined using the formula (3).

From the above, we can get: $m_c=8$, $m_r=6$, $r=16818$. According to the parameter design table, we can get: $m_0=6$, m_0 represents the experimental points when each factor was set as zero levels. From the above, the experiments' total number N can be determined using the equation (4):

$$N = m_c + m_r + m_0 = 20 \quad (4)$$

The experimental scheme design is shown in Table 3, and the simulation models were established according to this plan.

Performing experiments based on experimental conditions

Different FE models were generated through parametrically setting the controllable factors. The test was conducted based on the 15 FE models. The maximum Von Mises stress on the C5 inferior and C6 superior endplates of each model was collected and compared to define the optimal structural dimensional parameters of cage.

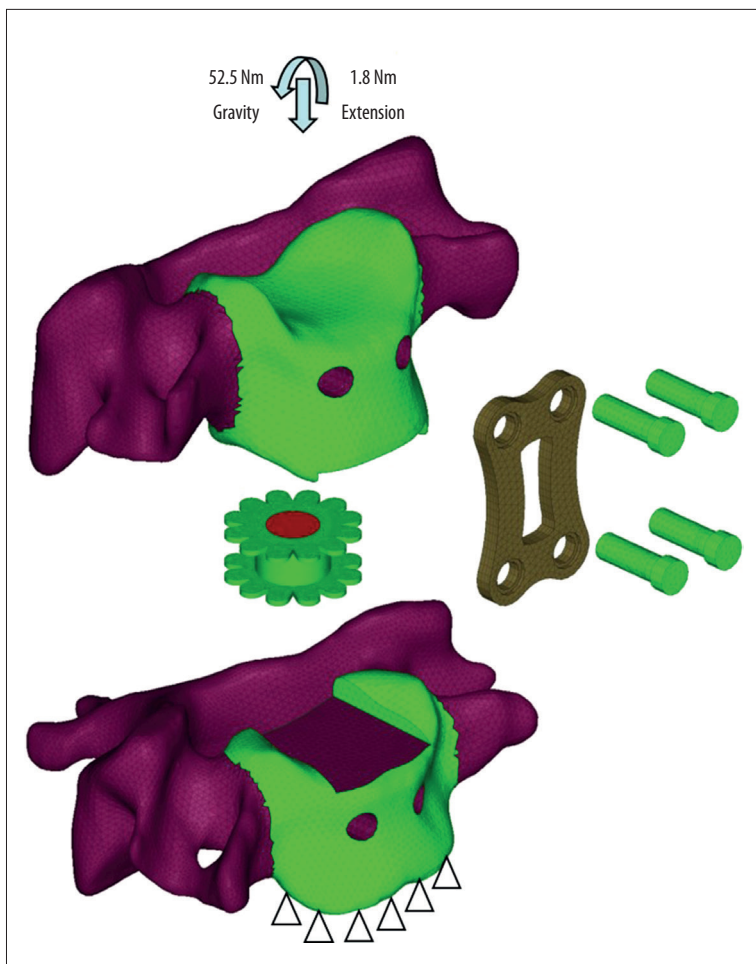


Figure 1. The C5–C6 FE model with cage implantation and its boundary and loading condition. A uniform compression force of 52.5 N mimicking the gravity of head, and a moment of 1.8 Nm mimicking the flexion motion pattern was exerted on the vertebrae of C5, while the nodes at the bottom of C6 were completely constrained.

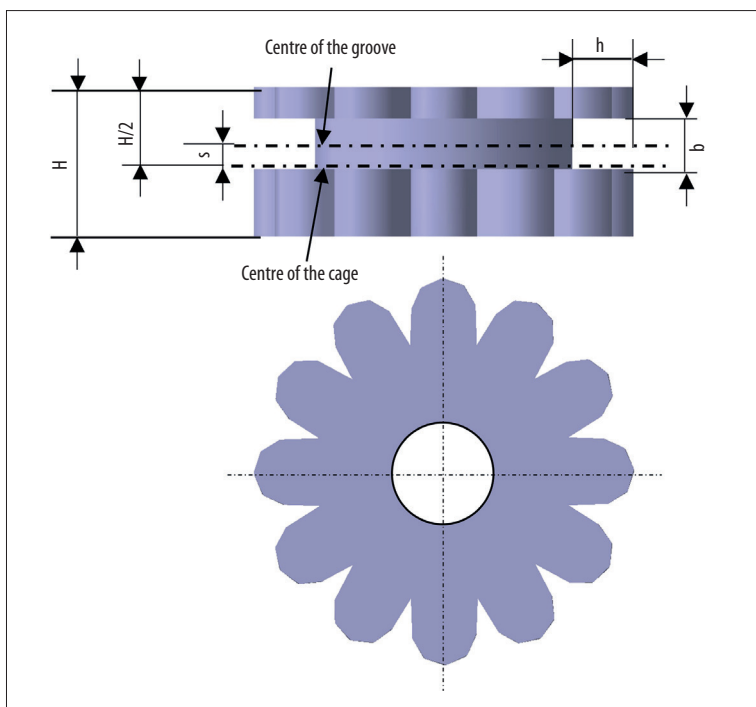


Figure 2. Schematic diagram of cervical cage's structural dimensions. H – Distance from the superior and inferior edge; s – Distance between the center of cage and center of groove; h – Depth of the groove; b – Width of the groove.

Table 2. Factor level coding table.

$x_1(z_1)$	z_1/mm	z^2/mm	z_3/mm
$R(z_{2j})$	1	2	2.5
$1(z_{0j}+\Delta_j)$	0.595	1.696	2.095
$0(z_{0j})$	0	1.25	1.5
$-1(z_{0j}-\Delta_j)$	-0.595	0.804	0.905
$-r(z_{1j})$	-1	0.5	0.5
$\Delta_j = \frac{z_{2j} - z_{1j}}{2r}$	0.595	0.446	0.595
$x_j = \frac{z_j - z_{0j}}{\Delta_j}$	$x_1 = \frac{(z_1 - 0)}{0.595}$	$x_2 = \frac{(z_2 - 1.25)}{0.446}$	$x_3 = \frac{(z_3 - 1.5)}{0.595}$

Table 3. Quadratic rotating experimental design scheme.

Factors No. of experiments	$x_1(z_1)$	$x_2(z_2)$	$x_3(z_3)$
1	1 (0.5946)	1 (1.696)	1 (2.0946)
2	1 (0.5946)	1 (1.696)	-1 (0.9054)
3	1 (0.5946)	-1 (0.804)	1 (2.0946)
4	1 (0.5946)	-1 (0.804)	-1 (0.9054)
5	-1 (-0.5946)	1 (1.696)	1 (2.0946)
6	-1 (-0.5946)	1 (1.696)	-1 (0.9054)
7	-1 (-0.5946)	-1 (0.804)	1 (2.0946)
8	-1 (-0.5946)	-1 (0.804)	-1 (0.9054)
9	-r (-1)	0 (1.25)	0 (1.5)
10	r (1)	0 (1.25)	0 (1.5)
11	0 (0)	-r (0.5)	0 (1.5)
12	0 (0)	r (2)	0 (1.5)
13	0 (0)	0 (1.25)	-r (0.5)
14	0 (0)	0 (1.25)	r (2.5)
15	0 (0)	0 (1.25)	0 (1.5)
16	0 (0)	0 (1.25)	0 (1.5)
17	0 (0)	0 (1.25)	0 (1.5)
18	0 (0)	0 (1.25)	0 (1.5)
19	0 (0)	0 (1.25)	0 (1.5)
20	0 (0)	0 (1.25)	0 (1.5)

The quadratic rotation regression analysis design method

The stress responses of all bionic optimal experimental tests were used for the regression analysis.

For the p-dimensional factor space, the regression equation is assumed as:

$$\hat{y} = b_0 + \sum_{j=1}^p b_j x_j + \sum_{h<j} b_{hj} x_h x_j + \sum_{j=1}^p b_{jj} x_j^2 \quad (5)$$

Regression coefficient analysis

When calculating the regression coefficient of quadratic rotation design, the formula is based on:

$$\left\{ \begin{array}{l} b_0 = K \sum_{i=1}^N y_i + E \sum_{j=1}^p \sum_{i=1}^N x_{ij}^2 y_i \\ b_j = e^{-1} \sum_{i=1}^N x_{ij} y_i = \frac{B_j}{D_j} \\ b_{hj} = m_c^{-1} \sum_{i=1}^N (x_{ih} x_{ij}) y_i = \frac{B_{hj}}{D_{hj}} \\ b_{jj} = E \sum_{i=1}^N y_i + \frac{1}{2} r^{-4} \sum_{i=1}^N x_{ij}^2 y_i + G \sum_{j=1}^p \sum_{i=1}^N x_{ij}^2 y_i \end{array} \right. \quad (6)$$

$$\left\{ \begin{array}{l} K = 2r^4 H^{-1} [f + (p - 1)m_c] \\ E = -2H^{-1} e r^4 \\ G = H^{-1} (e^2 - N m_c) \\ e = m_c + 2r^2 \\ f = m_c + 2r^4 \\ H = 2r^4 [Nf + (p - 1)N m_c - p e^2] \end{array} \right. \quad (7)$$

The significance test of the regression equation

In the significance test to the regression equation, we assume that $y_1, y_2, \dots, y_i, \dots, y_N$ are experimental data of quadratic rotation design, thus the sum of the deviation squares and degree of freedom is:

$$S = \sum_{i=1}^N y_i^2 - \frac{1}{N} (\sum_{i=1}^N y_i)^2 \quad (8)$$

$$f = N - 1 \quad (9)$$

$$S_R = \sum_{i=1}^N y_i^2 - b_0 B_0 - \sum_{j=1}^p b_j B_j - \sum_{\substack{h<j \\ \lambda \in \lambda^*}} b_{hj}^{(\lambda)} B_{hj} - \sum_{j=1}^p b_{jj} B_{jj} \quad (10)$$

$$f_R = N - 2p - \lambda^* - 1 \quad (11)$$

$$S_{reg} = S - S_R \quad (12)$$

$$f_{reg} = f - f_R = 2p + \lambda^* \quad (13)$$

$$S_e = \sum_{i_0=1}^{m_0} y_{i_0}^2 - \frac{1}{m_0} (\sum_{i_0=1}^{m_0} y_{i_0})^2 \quad (14)$$

$$f_e = m_0 - 1 \quad (15)$$

$$S_{lf} = S_R - S_e \quad (16)$$

$$f_{lf} = f_R - f_e \quad (17)$$

The significance test and the lack of fit test of the regression formula still use the F test as follows:

$$F_{reg} = \frac{S_{reg}/f_{reg}}{S_R/f_R} \sim F_{\alpha}(f_{reg}, f_R) \quad (18)$$

$$F_{lf} = \frac{S_{lf}/f_{lf}}{S_e/f_e} \sim F(f_{lf}, f_e) \quad (19)$$

The regression coefficient test using the t test is as follows:

$$\left\{ \begin{array}{l} D(b_0) = K\sigma^2, t_0 = |b_0|/\sqrt{K S_e/f_e} \sim t_{\alpha}(f_e) \\ D(b_i) = e^{-1}\sigma^2, t_j = |b_j|/\sqrt{e^{-1} S_e/f_e} \sim t_{\alpha}(f_e) \\ D(b_{hj}) = m_c^{-1}\sigma^2, t_{hj} = |b_{hj}|/\sqrt{m_c^{-1} S_e/f_e} \sim t_{\alpha}(f_e) \\ D(b_{jj}) = F\sigma^2, t_{jj} = |b_{jj}|/\sqrt{F S_e/f_e} \sim t_{\alpha}(f_e) \end{array} \right. \quad (20)$$

In this formula, the value of F can be obtained from formula (19) or referring to Table 4. If the regression equation matches, use S_R/f_R for S_e/f_e in formula (19) for the regression coefficient t test. The K, E, G can be calculated from formula (7) or directly looked up from Table 4.

The significance of each item of the regression equations on the test index were tested by the t test:

$$t(f_e) = |b_j|/\sqrt{D(b_j)} \sim t_{\alpha}(f_e) \quad (21)$$

If $t(f_e) > t_{\alpha}(f_e)$, the regression item tested can be considered as significant at the level α , and vice versa:

$$\left\{ \begin{array}{l} D(b_0) = K\sigma^2 = 0.1663\sigma^2 \\ t_0 = |b_0|/\sqrt{0.1663\sigma^2} \end{array} \right. \quad (22)$$

$$\left\{ \begin{array}{l} D(b_j) = e^{-1}\sigma^2 \\ t_j = |b_j|/\sqrt{e^{-1}\sigma^2}, j=1,2,3 \end{array} \right. \quad (23)$$

$$\left\{ \begin{array}{l} D(b_{hj}) = m_c^{-1}\sigma^2 \\ t_{hj} = |b_{hj}|/\sqrt{m_c^{-1}\sigma^2}, h<j; h, j \in 3 \end{array} \right. \quad (24)$$

$$\left\{ \begin{array}{l} D(b_{jj}) = F\sigma^2 \\ t_{jj} = |b_{jj}|/\sqrt{F\sigma^2}, jj=1, 2, 3 \end{array} \right. \quad (25)$$

Results

The optimization design simulation results

The values of all the results according to the quadratic rotation design layout were obtained. Fortunately, stress responses

Table 4. The quadratic regression general rotation design parameter [21].

p	$p_c = \sqrt{p}$	$m_c = 2^{p-1}$	$m_r = 2p$	m_o	N	λ_4	K	-E	F	G
2	1.414	4	4	5	13	0.813	0.2000	0.1000	0.1438	0.0188
3	1.732	8	6	6	20	0.857	0.1663	0.0568	0.0684	0.0069
4	2.000	16	8	7	31	0.861	0.1428	0.0357	0.0350	0.0037

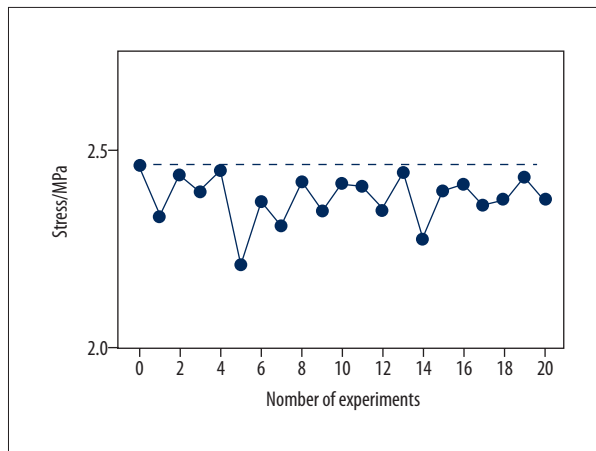


Figure 3. The comparison between Von Mises stresses of the original structural cage (the black dotted line) and bionic structural ones using quadratic rotation design (the blue polyline).

distributing at the endplates of bionic structural cages' simulation results were all lower than before (Figure 3).

Regression coefficient analysis

According to formulas (6) and (7), we calculated the regression coefficients. The value of F, K, E, G were obtained using Table 4. We calculated the regression coefficient such as b_0 , b_{jj} as follows:

$$b_0 = 0.1663 \sum_{i=1}^{20} y_i - 0.0568 \sum_{j=1}^3 \sum_{i=1}^{20} x_{ij}^2 y_i = 2.39222$$

$$b_{jj} = -0.0568 \sum_{i=1}^{20} y_i + \frac{1}{2} r^{-4} \sum_{i=1}^{20} x_{ij}^2 y_i + 0.0069 \sum_{j=1}^3 \sum_{i=1}^{20} x_{ij}^2 y_i$$

Then, we can get:

$$b_{11} = -2.0139 + 0.0625B_{11} = -0.4795,$$

$$b_{22} = -2.0139 + 0.0625B_{22} = -0.0534,$$

$$b_{33} = -2.0139 + 0.0625B_{33} = -0.0603.$$

The calculation results of the above regression coefficients are listed in Table 5.

Among these coefficients, the values of $x_1 x_2$ and $x_2 x_3$ are close to zero and can be neglected. Then, the regression equation can be simplified as follows:

$$\hat{y} = 2.3922 + 0.0313x_1 - 0.0237x_2 - 0.0522x_3 + 0.0144x_1 x_3 - 0.4795x_1^2 - 0.0534x_2^2 - 0.0603x_3^2$$

The significance test of the regression equation

Before the significance analysis, various squares sum of deviations and degree of freedom are calculated as follows according to formula (8–17):

$$S = \sum_{i=1}^{20} y_i^2 - \frac{1}{20} (\sum_{i=1}^{20} y_i)^2 = 112.8877 - 112.8173 = 0.0704,$$

$$f = N - 1 = 19,$$

$$S_R = \sum_{i=1}^{20} y_i^2 - b_0 B_0 - \sum_{j=1}^3 b_j B_j - \sum_{h < j} b_{hj} B_{hj} - \sum_{j=1}^3 b_{jj} B_{jj} = 0.0054,$$

$$S_{reg} = S - S_R = 0.0065,$$

$$f_{reg} = 9,$$

$$f_R = f - f_{reg} = 10,$$

$$S_e = \sum_{i=0}^6 (y_{i_0} - \bar{y}_0)^2 = 0.0037,$$

$$f_e = 6 - 1 = 5,$$

$$S_{lf} = S_R - S_e = 0.0016,$$

$$f_{lf} = f_R - f_e = 5.$$

The significance test of the regression formula used the F test, carried out according to formula (18) and (19) as follows:

The loss of quasi inspection:

$$F_{lf} = \frac{S_{lf}/f_{lf}}{S_e/f_e} = \frac{0.0016/5}{0.0037/5} = 0.4324 < F_{0.25}(5,5) = 1.89$$

Thus, the regression equation did not lose quasi:

$$F_{reg} = \frac{S_{reg}/f_{reg}}{S_R/f_R} = \frac{0.0065/9}{0.0054/10} = 1.3374 < F_{0.25}(9,10) = 1.56$$

However, the regression equation is not significant.

Among them, $\sigma^2 = S_R/f_R = 0.0054/10 = 0.00054$.

The *t* test results are listed in Table 5. The items of b_1 , b_2 , b_3 , b_3^2 have significant effects on different degrees. To obtain the

Table 5. The calculation results of regression coefficients.

No.	x_0	$x_1(z_1)$	$x_2(z_2)$	$x_3(z_3)$	x_1x_2	x_1x_3	x_2x_3	x_1^2	x_2^2	x_3^2	y_i
1	1	1 (0.595)	1 (1.696)	1 (2.0946)	1	1	1	1	1	1	2.332
2	1	1 (0.5946)	1 (1.696)	-1 (0.9054)	1	-1	-1	1	1	1	2.437
3	1	1 (0.5946)	-1 (0.804)	1 (2.0946)	-1	1	-1	1	1	1	2.396
4	1	1 (0.5946)	-1 (0.804)	-1 (0.9054)	-1	-1	1	1	1	1	2.448
5	1	-1 (-0.5946)	1 (1.696)	1 (2.0946)	-1	-1	1	1	1	1	2.208
6	1	-1 (-0.5946)	1 (1.696)	-1 (0.9054)	-1	1	-1	1	1	1	2.369
7	1	-1 (-0.5946)	-1 (0.804)	1 (2.0946)	1	-1	-1	1	1	1	2.307
8	1	-1 (-0.5946)	-1 (0.804)	-1 (0.9054)	1	1	1	1	1	1	2.418
9	1	-1.6818 (-1)	0 (1.25)	0 (1.5)	0	0	0	2.8284	0	0	2.346
10	1	r (1)	0 (1.25)	0 (1.5)	0	0	0	0	0	0	2.415
11	1	0 (0)	-1.6818 (0.5)	0 (1.5)	0	0	0	0	2.8284	0	2.408
12	1	0 (0)	1.6818 (2)	0 (1.5)	0	0	0	0	2.8284	0	2.348
13	1	0 (0)	0 (1.25)	-1.6818 (0.5)	0	0	0	0	0	2.8284	2.443
14	1	0 (0)	0 (1.25)	1.6818 (2.5)	0	0	0	0	0	2.8284	2.274
15	1	0 (0)	0 (1.25)	0 (1.5)	0	0	0	0	0	0	2.396
16	1	0 (0)	0 (1.25)	0 (1.5)	0	0	0	0	0	0	2.414
17	1	0 (0)	0 (1.25)	0 (1.5)	0	0	0	0	0	0	2.359
18	1	0 (0)	0 (1.25)	0 (1.5)	0	0	0	0	0	0	2.377
19	1	0 (0)	0 (1.25)	0 (1.5)	0	0	0	0	0	0	2.432
20	1	0 (0)	0 (1.25)	0 (1.5)	0	0	0	0	0	0	2.374
D_j	20	13.6569	13.6569	13.6569	8	8	8	15.9998	23.9997	23.9997	225.7753
B_j	47.501	0.4270442	-0.3239	-0.7132	0.073	0.115	-0.103	25.5504	32.3669	32.2566	
b_j	2.3922	0.0313	-0.0237	-0.0522	0.0091	0.0144	-0.00129	-0.4795	-0.0534	-0.0603	
b_jB_j	113.6319	0.0134	0.0077	0.0372	0.0007	0.0017	0.0013	-12.2506	-1.7297	-1.9461	
t_j	252.4379	2.2200	1.6815	3.7036	0	0.0001	0.0001	0.0029	0.0003	0.0004	
a_j	0.001	0.1	0.2	0.02	-	-	-	-	-	-	

lower stress response of the endplate, the factors which have a significant effect were put into the equation, so the regression equation can be described as follows:

$$\hat{y} = 2.3922 + 0.0313x_1 - 0.0237x_2 - 0.0522x_3$$

According to the relationship formula between z_1, z_2, z_3 and x_1, x_2, x_3 , the x_1, x_2, x_3 are all replaced using z_1, z_2, z_3 , the equation could be changed as:

To ensure the formation of the groove structure, the width of the groove and the location of the groove should meet the condition as equation as follows, namely $2.5 - (|s| + \frac{b}{2}) \geq 0.5$, namely $|s| + \frac{b}{2} \leq 2$.

The depth of the groove is relative to the radius of the cage itself and the radius of center opening. The radius of the cage was 6.5 mm, the radius of the center opening was 2.5 mm. Thus, after processing groove structure, the thickness of cage (h') radially should not less than 1 mm to ensure the cage's minimum size. Specifically, $h' = 6.5 - 2.5 - h \geq 1$, thus the groove should meet $0 \leq h \leq 3$.

From the discussion above, the groove size optimum problem can be represented using the following equations:

$$\left\{ \begin{array}{l} \sigma = 2.5902 + 0.0526s - 0.0531b - 0.0877h \\ |s| + \frac{b}{2} \leq 2 \\ b \geq 0 \\ |s| \geq 0 \\ 0 \leq h \leq 3 \end{array} \right.$$

From the regression equation, the stress response of endplate is positively correlated to the s , the larger of value of s , the larger of stress response of endplate; the stress response of endplate is negatively correlated to the value of b and h , the larger of the value of b or h , the smaller of stress response of endplate. According to the equation (28), the optimum structural size parameters for minimum stress response of endplate were $s=0$ mm, $b=4$ mm, $h=3$ mm, respectively, and the minimum stress response of endplate was 2.1147 MPa. In order to validate the regression results, the cage designed using the size of the optimum parameter was simulated under the same boundary and loading condition with the others, and the endplate's stress response obtained from the simulation was 1.90527 Mpa, which was lower than the value calculated by the regression equation. Moreover, the stress response of endplate has decreased by 22.58% compared with the original one. The stress distribution on endplates, cages, bone grafts, and cancellous and cortical bone of C5 and C6 for the original cage and optimum structural cage were contrasted (Figures 4, 5).

Discussion

In this study, a cage with bionic structure was designed and optimized. As a result, the front view of the bionic structural cage is I-shaped. Because a previous study demonstrated that the contact area between cages and the endplates influenced the stress of endplates [24], in the present study, the same surface area of all cages with bionic structure was set to weaken the influence of cage surface area. Optimization was carried out based on the experimental optimum design idea [25]. Testing with only 20 runs using the regression analysis method reduces the test number and improves the efficiency of exploring optimization parameters.

In addition, the relationship between the 3 structural size parameters of the cervical cage and the end plate stress was proved using regression analysis theory. The results showed that a cage with a lower distance between the center of the cage and groove and higher depth and width of the groove produced a lower stress response on the endplate. According to the simulation results, the regression formula showed that all the structural factors demonstrated in this work took part in influencing the stress responses of endplates. Furthermore, the results show that the optimization target changes linearly with the change of factors. The distance between the center of the cage and groove has a positive effect on the stress response of the endplate; nevertheless, both the depth and width of the groove have negative effects.

To understand the influence mechanism of the structural design compared to the original one, the stress distribution was compared in Figures 4 and 5. As shown in Figure 4, the stresses distributed on the endplates was smaller and more uniform, which directly resist the occurrence of subsidence. Figure 5 showed that the new optimized structural cage changed the stress distribution state on the adjacent tissues. The stress was distributed mainly on the edge of the superior-inferior surfaces of vertebra of the original cage design, but it was mainly distributed on the center of the vertebra of the optimized design. This was conducive to the promotion of the cage's subsidence-resistance. In short, when using 3 variables that vary within a certain range for experimental design, a regression analysis method can be effectively used to explore the relationship between these structural parameters and the target stress response. In addition, the experimental optimization design method can improve the consistency of experimental design and analysis and can reduce the experimental time and cost. Because there are many products or processes in the field of biomechanics that require optimal implementation, regression analysis methods could make a huge contribution.

This study has some limitations. The model established in this study sets the material properties of vertebrae, bone grafts,

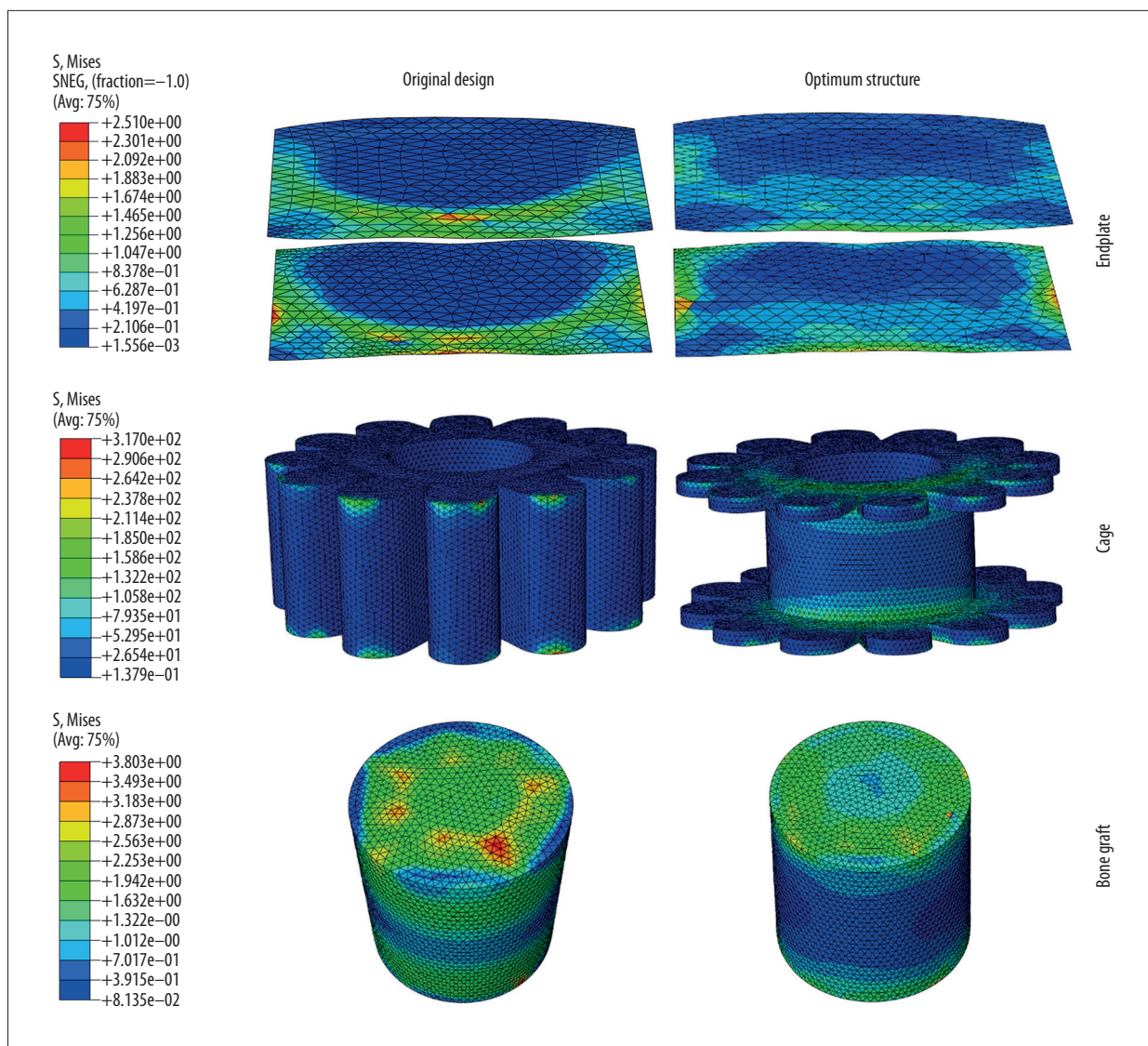


Figure 4. The stress distribution on endplates, cages, and bone grafts for original cage and optimum structural one.

and cages to be isotropic linear. Furthermore, the screws were set as solid cylinders in combination with vertebrae and plates, and the screw threads were not modeled in the analysis [36]. Theoretically, by keeping the test conditions of all the surgical models consistent, the results obtained from the FE analysis can be taken as an effective method to demonstrate the biomechanical properties related to the bionic structure design of the cervical anterior surgical cage.

Conclusions

In the study, the influence of bionic structural design of cervical intervertebral cage on the postoperative effects was investigated. The simulation results showed that cages with bionic structure design could effectively decrease the stress response

of endplate, which improved the subsistence property. By using secondary rotation regression optimization design and analysis method, the regression equations were developed between stress responses of endplate and the structural sized parameters. Furthermore, the equation could significantly predict the value of the optimum object (the stress response of endplate) through significance analysis of the equation. The simulation model established using the cage with optimization parameters calculated the stress response of endplate matched well with the prediction of the regression equation. Our results suggest that the optimization method has great potential application in the biomechanical engineering field.

Conflicts of interest

None.

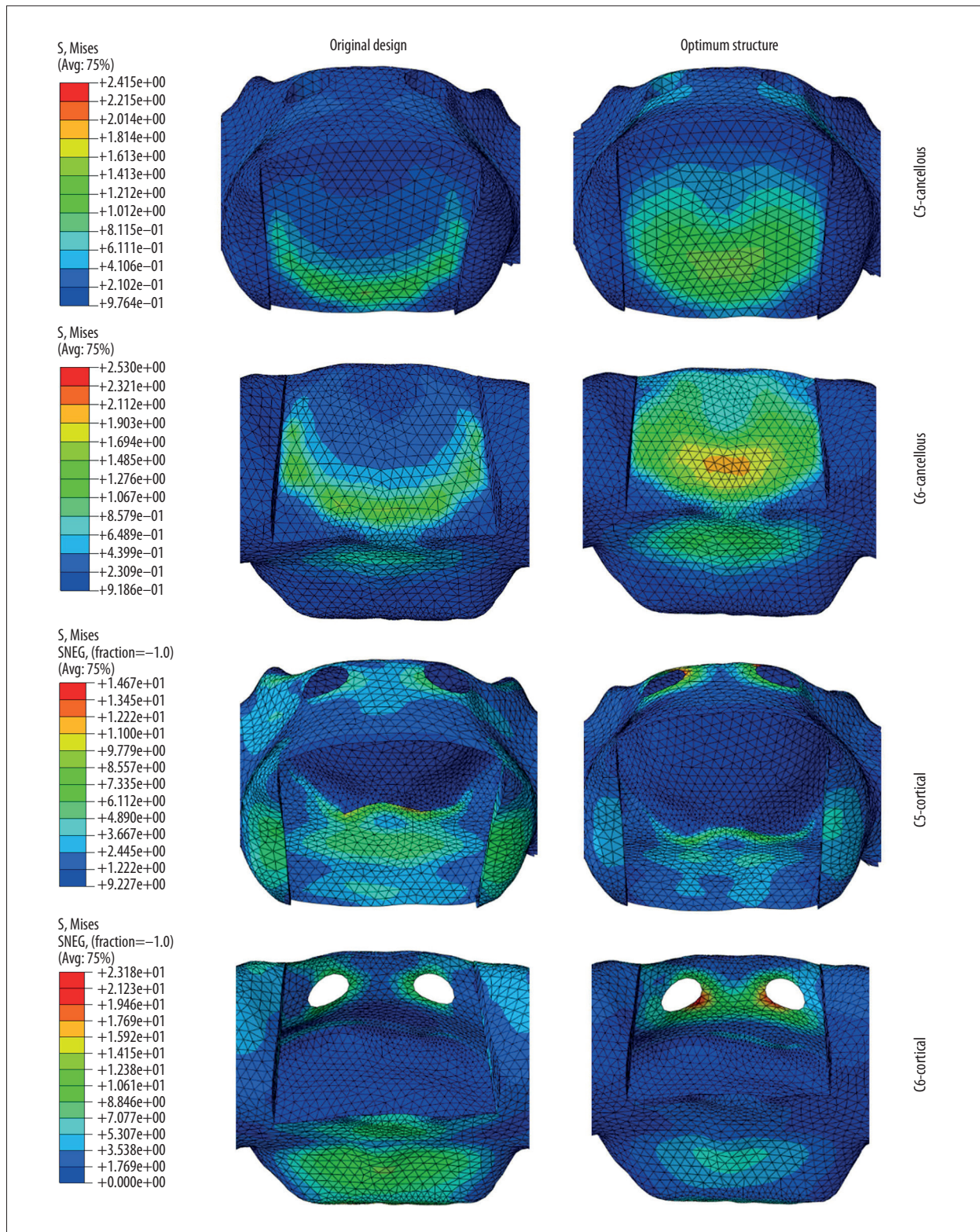


Figure 5. The stress distribution on cancellous and cortical bone of C5 and C6 for the original cage and optimum structural one.

References:

- Liu C, Liu KX, Chu L et al: Posterior percutaneous endoscopic cervical discectomy through lamina-hole approach for cervical intervertebral disc herniation. *Int J Neurosci*, 2019; 129: 627–34
- Balasa A, Bielecki M, Prokopenko M, Kunert P: Lateral approach for recurrent unilateral cervical radiculopathy after anterior discectomy with fusion. Report of two cases. *Videosurgery Miniinv*, 2019; 14: 348–52
- Eco LC, Brayton A, Whitehead WE, Jea A: Reconstruction of the anterior craniocervical junction using an expandable cage after resection of a C1 chordoma in a 5-year-old child: Case report. *J Neurosurg-Pediatr*, 2019; 24: 62–65
- Alvi MA, Kurian SJ, Wahood W et al: Assessing the difference in clinical and radiologic outcomes between expandable cage and nonexpandable cage among patients undergoing minimally invasive transforaminal interbody fusion: A systematic review and meta-analysis. *World Neurosurg*, 2019; 127: 596–606.e1
- Goz V, Buser Z, D'Oro A et al: Complications and risk factors using structural allograft versus synthetic cage: Analysis 17783 anterior cervical discectomy and fusions using a national registry. *Global Spine J*, 2019; 9: 388–92
- Wilke H J, Kettler A, Goetz C, Claes L: Subsidence resulting from simulated postoperative neck movements: An *in vitro* investigation with a new cervical fusion cage. *Spine*, 2000; 25(21): 2762–70
- Kandziora F, Pflugmacher R, Schäfer J et al: Biomechanical comparison of cervical spine interbody fusion cages. *Spine*, 2001; 26(17): 1850–57
- Kandziora F, Schollmeier G, Scholz M et al: Influence of cage design on interbody fusion in a sheep cervical spine model. *J Neurosurg*, 2002; 96(3): 321–32
- Kandziora F, Pflugmacher R, Scholz M et al: Bioabsorbable interbody cages in a sheep cervical spine fusion model. *Spine*, 2004; 29(17): 1845–55
- Oliver JD, Goncalves S, Kerezoudis P et al: Comparison of outcomes for anterior cervical discectomy and fusion with and without anterior plate fixation: A systematic review and meta-analysis. *Spine*, 2018; 43(7): E413–22
- Fernandez-Fairen M, Alvarado E, Torres A: Eleven-year follow-up of two cohorts of patients comparing stand-alone porous tantalum cage versus autologous bone graft and plating in anterior cervical fusions. *World Neurosurg*, 2019; 122: E156–67
- Noordhoek I, Koning MT, Vleggeert-Lankamp CLA: Evaluation of bony fusion after anterior cervical discectomy: A systematic literature review. *Eur Spine J*, 2019; 28(2): 386–99
- Kettler A, Wilke HJ, Claes L: Effects of neck movements on stability and subsidence in cervical interbody fusion: An *in vitro* study. *J Neurosurg*, 2001; 94(1 Suppl): 97–107
- Lu T, Liang H, Liu C et al: Effects of titanium mesh cage end structures on the compressive load at the endplate interface: A cadaveric biomechanical study. *Med Sci Monit*, 2017; 23: 2863–70
- Mao CY, Ma YH, Wu SY et al: Wear resistance and wet skid resistance of composite bionic tire tread compounds with pit structure. *Mater Res Express*, 2019; 6: 085331
- Li KY, Yang XY, Xue C et al: Biomimetic human lung-on-a-chip for modeling disease investigation. *Biomicrofluidics*, 2019; 13(3): 031501
- Wang M, Dong HF, Li X et al: Control and optimization of a bionic robotic fish through a combination of CPG model and PSO. *Neurocomputing*, 2019; 337: 144–52
- Wang J, Du ZZ, He ZT, Wang JJ: Exploring vibration transmission rule of an artificial spider web for potential application in invulnerability of wireless sensor network. *Appl Bionics Biomech*. 2019; 2019: 5125034
- Mohanty S, Dahia CL: Defects in intervertebral disc and spine during development, degeneration, and pain: New research directions for disc regeneration and therapy. *Wires Dev Biol*, 2019; 8(4): e343
- Zhao RZ, Liu WQ, Xia TT, Yang L: Disordered mechanical stress and tissue engineering therapies in intervertebral disc degeneration. *Polymers*, 2019; 11(7): 1151
- Kuo RF, Fang KM, Wong TY, Hu CY: Quantification of dental prostheses on cone-beam CT images by the Taguchi method. *J Appl Clin Med Phys*, 2016; 17: 207–20
- Usma-Alvarez CC, Fuss FK, Subic A: User-centered design customization of rugby wheelchairs based on the Taguchi method. *J Mech Design*, 2014; 136(4): 041001
- Fan CY, Chao CK, Hsu CC, Chao KH: The optimum cage position and orientation on the ALIF with facet screw fixation: A finite element analysis and the Taguchi method. *J Mech*, 2011; 27(3): 309–20
- Yang K, Teo EC, Fuss FK: Application of Taguchi method in optimization of cervical ring cage. *J Biomech*, 2007; 40: 3251–56
- Ren LQ: [Regression design and optimization.] 1th ed. Beijing (NY): Science Press; 2009 [in Chinese]
- Wang J, Qian Z, Ren L: Biomechanical comparison of optimal shapes for the cervical intervertebral fusion cage for C5–C6 cervical fusion using the Anterior Cervical Plate and Cage (ACPC) fixation system: A finite element analysis. *Med Sci Monit*, 2019; 25: 8379–88
- Zhang QH, Teo EC, Ng HW, Lee VS: Finite element analysis of moment-rotation relationships for human cervical spine. *J Biomech*, 2006; 39: 189–93
- Ha SK: Finite element modeling of multi-level cervical spinal segments (C3–C6) and biomechanical analysis of an elastomer-type prosthetic disc. *Med Eng Phys*, 2006; 28: 534–41
- Ng HW, Teo EC: Nonlinear finite-element analysis of the lower cervical spine (C4–C6) under axial loading. *J Spinal Disord*, 2001; 14: 201–10
- Kallemeyn N, Gandhi A, Kode S et al: Validation of a C2–C7 cervical spine finite element model using specimen-specific flexibility data. *Med Eng Phys*, 2010; 32: 482–89
- Panzer MB, Cronin DS: C4–C5 segment finite element model development, validation, and load-sharing investigation. *J Biomech*, 2009; 42: 480–90
- Teo EC, Yang K, Fuss FK et al: Effects of cervical cages on load distribution of cancellous core—a finite element analysis. *J Spinal Disord Tech*, 2004; 17(3): 226–31
- Natarajan RN, Chen BH, An HS, Andersson GBJ: Anterior cervical fusion: A finite element model study on motion segment stability including the effect of osteoporosis. *Spine*, 2000; 25(8): 955–61
- Reilly DT, Burstein AH, Frankel VH: The elastic modulus for bone. *J Biomech*, 1974; 7: 271–75
- Yang K, Teo EC, Fuss FK: Application of Taguchi method in optimization of cervical ring cage. *J Biomech*, 2007; 40: 3251–56
- Meng L, Zhang Y, Lu Y: Three-dimensional finite element analysis of mini-external fixation and Kirschner wire internal fixation in Bennett fracture treatment. *Orthop Traumatol Surg Res*, 2013; 99(1): 21–29